

Supporting Information for

Oxaziridine Cleavage with a Low-Valent Nickel Complex: Competing C-O and C-N Fragmentation

Addison N. Desnoyer,* Weiling Chiu, Candy Cheung, Brian O. Patrick and Jennifer A. Love*

Department of Chemistry, The University of British Columbia, Vancouver, British Columbia,
Canada V6T 1Z1

E-mail: jenlove@chem.ubc.ca

Table of Contents

I. General Considerations	S1
II. Organometallic Syntheses	S3
III. Mechanistic Scheme	S6
IV. NMR spectra	S8
V. UV/vis Spectrophotometry	S21
VI. X-ray Crystallography	S26

I. General Considerations: Unless stated otherwise, all reactions were performed in a glovebox or on a Schlenk line under an atmosphere of pure N₂ using standard Schlenk techniques. Anhydrous pentanes, toluene, diethyl ether, benzene, hexanes and tetrahydrofuran were purchased from Aldrich, sparged with N₂, and dried further by passage through towers containing activated alumina and molecular sieves. Toluene-d₈, C₆D₆ and THF-d₈ were purchased from Aldrich and dried over sodium/benzophenone before being distilled and degassed by three freeze-pump-thaw cycles. Arene dimer **1** was prepared according to the literature procedure.¹ Oxaziridines **2**² and **7**,³ imines **5**⁴ and **10**,³ and amides **6**⁵ and **11**⁶ were prepared according to the literature procedures. Imido complex **9** was prepared according to the procedure of Waterman and Hillhouse.⁷ ¹⁵N-labelled adamantylamine was prepared according to the literature procedure⁸ using ¹⁵N-labelled urea. All other chemicals were purchased from commercial suppliers and used as received.

NMR spectra were recorded on 300, 400 and 600 MHz spectrometers and are referenced to residual protio solvent (7.16 ppm for C₆D₅H, 2.08 ppm for C₆D₅CD₂H) for ¹H NMR spectroscopy, solvent peaks (128.06 ppm for C₆D₆, 20.43 ppm for C₆D₅CD₂H) for ¹³C NMR spectroscopy. ³¹P{¹H} NMR spectra were referenced to 85 % H₃PO₄ at 0 ppm. Quantitative ¹H NMR data were acquired with a minimum of eight scans, with the delay time set to 5x the longest T₁ value present, using 1,3,5-trimethoxybenzene as an internal standard. Quantitative ³¹P{¹H} NMR data were acquired using inverse gated experiments,⁹ with the delay time set to 5x the longest T₁ value present, using OPEt₃ as an internal standard. NMR spectra were taken at 25°C unless otherwise noted. Mass spectra and elemental analyses were performed by the microanalytic services in the Department of Chemistry at the University of British Columbia. HPLC-MS analyses were conducted using a Poroshell 120 SB-C18, 2.1 x 50 mm, 2.7 Micron

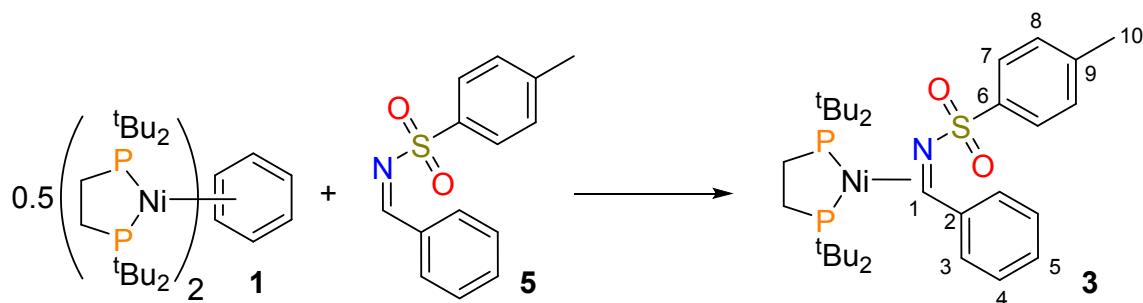
Column and the following conditions – flow rate = 0.650 mL/min; 35 °C; 2 µL; solvent A = water + 0.10% TFA; solvent B = MeCN + 0.10% TFA; pump method: 0 min, 10% B, 0.1 min 20% B, 2.3-3.3 min, 100% B. UV-Vis spectrophotometry was performed between wavelengths of 200 and 800 nm with an anaerobic quartz cell with a 1 cm path length.

References

1. I. Bach; K.-R. Porschke; R. Goddard; C. Kopsiske; C. Kruger; A. Rufinska; K. Seevogel *Organometallics* 1996, **15**, 4959-4966.
2. F. A. Davis; J. Lamendola; U. Nadir; E. W. Kluger; T. C. Sedergran; T. W. Panunto; R. Billmers; R. Jenkins; I. J. Turchi *J. Am. Chem. Soc.* 1980, **102**, 2000-2005.
3. R. Braslau; G. O'Bryan; A. Nilsen; J. Henise; T. Thongpaisanwong; E. Murphy; L. Mueller; J. Ruehl *Synthesis* 2005, 1496-1506.
4. J. Novacek; L. Roiser; K. Zielke; R. Robiette; M. Waser *Chem. Eur. J.* 2016, **22**, 11422-8.
5. F. Peron; C. Fossey; J. Sopkova-de Oliveira Santos; T. Cailly; F. Fabis *Chem. Eur. J.* 2014, **20**, 7507-13.
6. T. Zhang; Z. Wang; X. Hu; M. Yu; T. Deng; G. Li; H. Lu *J. Org. Chem.* 2016, **81**, 4898-905.
7. R. Waterman; G. L. Hillhouse *J. Am. Chem. Soc.* 2008, **130**, 12628-9.
8. E. Shokova *Synthesis* 1997, **1997**, 1034-1040.
9. B. Procacci; Y. Jiao; M.E. Evans; W.D. Jones; R.N. Perutz; A.C. Whitwood *J Am. Chem. Soc.* 2015, **137**, 1258-72.

II. Organometallic Syntheses

Synthesis of **3**



To a red-orange solution of **1** (36.7 mg, 0.0441 mmol, 1.0 equiv) in 4 mL of Et₂O was dropwise added a solution of imine **5** (23.7 mg, 0.0914 mmol, 2.1 equiv) in 4 mL of Et₂O, resulting in a colour change to red. The solution was then stirred at room temperature for 2 hours. The volatiles were removed *in vacuo* to give a red residue, which was extracted with a minimum amount of Et₂O and filtered through glass fiber to give a red-orange solution. On standing at -30°C overnight, red crystals formed. The supernatant was decanted, and the solids were dried *in vacuo* to yield 40.2 mg (72% yield) of **3** as X-ray quality crystals.

¹H NMR (400 MHz, C₆D₆) δ 8.16 (d, *J*_{H,H} = 8.2 Hz, 2H, **H7**), 7.56 (d, *J*_{H,H} = 6.9 Hz, 2H, **H8**), 7.02 (t, *J*_{H,H} = 7.6 Hz, 2H, **H4**), 6.92 (m, 1H, **H5**), 6.65 (d, *J*_{H,H} = 8.1 Hz, 2H, **H3**), 4.90 (dd, *J*_{H,P} = 7.0 Hz, *J*_{H,P} = 2.0 Hz, 1H, **H1**), 1.70 (s, 3H, **H10**), 1.51 (d, *J*_{H,P} = 12.2 Hz, 9H, C(CH₃)₃), 1.47 (d, *J*_{H,P} = 12.0 Hz, 9H, C(CH₃)₃), 1.28 (d, *J*_{H,P} = 12.4 Hz, 9H, C(CH₃)₃), 0.61 (d, *J*_{H,P} = 12.1 Hz, 9H, C(CH₃)₃). Although the resonances for the methylene groups of the phosphine backbone were obscured, they could be detected indirectly through an HSQC experiment around 1.38 ppm and 1.20 ppm.

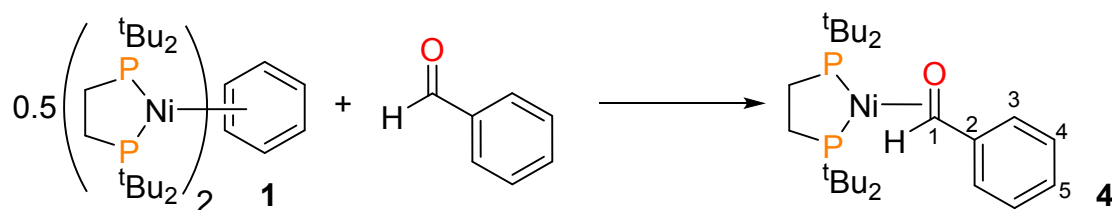
³¹P NMR (162 MHz, C₆D₆) δ 85.12 (d[AB], *J*_{P,P} = 44 Hz), 84.17 (d[AB], *J*_{P,P} = 43 Hz).

$^{13}\text{C}\{^1\text{H}\}$ NMR (100 MHz, C_6D_6) δ 148.3 (s, C2 or C6), 143.45 (s, C2 or C6), 140.29 (s), 128.93 (s), 128.35 (overlapping with the solvent signal, was detected indirectly using an HSQC experiment), 127.11 (s), 126.16 (s), 124.30 (s), 55.90 (d, $J_{\text{C,P}} = 27$ Hz, C1), 35.85 (dd, $J_{\text{C,P}} = 15$ Hz, $J_{\text{C,P}} = 2$ Hz, C(CH₃)₃), 35.14 (dd, $J_{\text{C,P}} = 14$ Hz, $J_{\text{C,P}} = 4$ Hz, C(CH₃)₃), 34.89 (dd, $J_{\text{C,P}} = 9$ Hz, $J_{\text{C,P}} = 3$ Hz, C(CH₃)₃), 34.51 (d, $J_{\text{C,P}} = 11$ Hz, C(CH₃)₃), 31.20 (d, $J_{\text{C,P}} = 5$ Hz, C(CH₃)₃), 30.91 (d, $J_{\text{C,P}} = 7$ Hz, C(CH₃)₃), 30.82 (d, $J_{\text{C,P}} = 6$ Hz, C(CH₃)₃), 29.85 (d, $J_{\text{C,P}} = 5$ Hz, C(CH₃)₃), 23.62 (app. t, $J_{\text{C,P}} = 17$ Hz, PCH₂CH₂P), 21.82 (dd, $J_{\text{C,P}} = 16$ Hz, $J_{\text{C,P}} = 13$ Hz, PCH₂CH₂P), 20.96 (s, C10).

Anal. Calcd: C, 60.39; H, 8.39; N, 2.20; Found: C, 60.01; H, 8.45; N, 2.12.

LRMS (EI) 635 [M^+]

Synthesis of 4



To a red-orange solution of **1** (48.6 mg, 0.0584 mmol, 1.0 equiv) in 4 mL of Et₂O was dropwise added a solution of benzaldehyde (18.9 mg, 0.178 mmol, 3.0 equiv) in 4 mL of Et₂O, resulting in a colour change to orange-yellow. The solution was then stirred at room temperature for 2 hours. The volatiles were removed *in vacuo* to give an orange residue, which was extracted with a minimum amount of Et₂O and filtered through glass fiber to give an orange-yellow solution. On

standing at -30°C overnight, red crystals formed. The supernatant was decanted, and the solids were dried *in vacuo* to yield 51.3 mg (91% yield) of **4** as X-ray quality crystals.

^1H NMR (400 MHz, C_6D_6) δ 7.78 (d, $J_{\text{H,H}} = 7.3$ Hz, 2H, **H3**), 7.21 (t, $J_{\text{H,H}} = 7.6$ Hz, 2H, **H4**), 7.09 (t, $J_{\text{H,H}} = 7.3$ Hz, 1H, **H5**), 5.87 (dd, $J_{\text{H,P}} = 6.3, 4.2$ Hz, 1H, **H1**), 1.30 (d, $J_{\text{H,P}} = 9.8$ Hz, 9H, $\text{C}(\text{CH}_3)_3$), 1.28 (d, $J_{\text{H,P}} = 9.8$ Hz, 9H, $\text{C}(\text{CH}_3)_3$), 1.17 (d, $J_{\text{H,P}} = 12.1$ Hz, 9H, $\text{C}(\text{CH}_3)_3$), 0.73 (d, $J_{\text{H,P}} = 12.3$ Hz, 9H, $\text{C}(\text{CH}_3)_3$). Although the methylene resonances of the phosphine backbone could not be resolved, they were detected indirectly *via* an HSQC experiment at around 1.37 and 1.31 ppm.

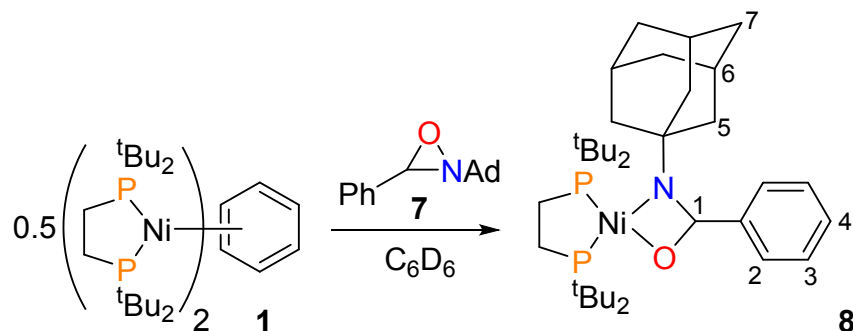
$^{31}\text{P}\{^1\text{H}\}$ NMR (162 MHz, C_6D_6) δ 90.0 (d[AB], $J_{\text{P,P}} = 71$ Hz), 88.2 (d[AB], $J_{\text{P,P}} = 71$ Hz).

$^{13}\text{C}\{^1\text{H}\}$ NMR (100 MHz, C_6D_6) δ 152.3 (d, $J_{\text{C,P}} = 6$ Hz, **C2**), 128.4 (d, $J_{\text{C,P}} = 3$ Hz, **C3**), 124.0 (d, $J_{\text{C,P}} = 3$ Hz, **C4**), 123.6 (d, $J_{\text{C,P}} = 3$ Hz, **C5**), 79.0 (d, $J_{\text{C,P}} = 21$ Hz, **C1**), 34.9 (dd, $J_{\text{C,P}} = 13$ Hz, $J_{\text{C,P}} = 5$ Hz, $\text{C}(\text{CH}_3)_3$), 34.6 (dd, $J_{\text{C,P}} = 12$ Hz, $J_{\text{C,P}} = 4$ Hz, $\text{C}(\text{CH}_3)_3$), 34.2 (dd, $J_{\text{C,P}} = 8$, $J_{\text{C,P}} = 4$ Hz, $\text{C}(\text{CH}_3)_3$), 33.7 (dd, $J_{\text{C,P}} = 7$, $J_{\text{C,P}} = 2$ Hz, $\text{C}(\text{CH}_3)_3$), 30.9 (d, $J_{\text{C,P}} = 8$ Hz, $\text{C}(\text{CH}_3)_3$), 30.6 (d, $J_{\text{C,P}} = 6$ Hz, $\text{C}(\text{CH}_3)_3$), 30.4 (d, $J_{\text{C,P}} = 7$ Hz, $\text{C}(\text{CH}_3)_3$), 30.0 (d, $J_{\text{C,P}} = 6$ Hz, $\text{C}(\text{CH}_3)_3$), 24.6 (dd, $J_{\text{C,P}} = 21$ Hz, $J_{\text{C,P}} = 19$ Hz, $\text{PCH}_2\text{CH}_2\text{P}$), 20.7 (dd, $J_{\text{C,P}} = 14$, $J_{\text{C,P}} = 12$ Hz, $\text{PCH}_2\text{CH}_2\text{P}$).

Anal. Calcd: C, 62.13; H, 9.59. Found: C, 62.52; H, 9.66.

LRMS (EI) 482 [M^+]

Synthesis of **8**



A red-orange solution of **1** (34.2 mg, 0.0411 mmol, 1.0 equiv) in 6 mL of Et₂O and a solution of oxaziridine **7** (20.5 mg, 0.0803 mmol, 2.0 equiv) in 3 mL Et₂O were both chilled in the glovebox freezer at -30°C. After 20 minutes, the solutions were removed from the freezer, and the solution of **7** was quickly poured into the solution of **1**, causing an instant colour change to dark purple. The solution was returned to the freezer for 1 hour, then quickly filtered through glass fiber while cold to give a dark purple solution. Removal of the volatiles *in vacuo* yielded 45.0 mg (88% yield) of **8** as a dark purple powder. X-ray quality crystals were grown by cooling a concentrated Et₂O solution of **8** at -30°C overnight. Complex **8** was found to be unstable even in the solid state at -30°C, decomposing to a mixture of compounds, including **4**, **9** and **10** after several days.

Due to the thermal instability of **8**, we were unable to achieve satisfactory analytic data.

¹H NMR (400 MHz, tol-d₈) δ 7.94 (d, *J*_{H,H} = 7.8 Hz, 2H, **H2**), 7.41 (t, *J*_{H,H} = 7.6 Hz, 2H, **H3**), 7.19 (t, *J*_{H,H} = 7.4 Hz, 1H, **H4**), 6.78 (br. s, 1H, **H1**), 2.53 (br. d, *J*_{H,H} = 11.7 Hz, 3H, **H5**), 2.29 (br. d, *J*_{H,H} = 11.7 Hz, 3H, **H5**), 2.19 (br. s, 3H, **H6**), 1.81 (br. d[AB], *J*_{H,H} = 11.7 Hz, 3H, **H7**), 1.74 (br. d[AB], *J*_{H,H} = 11.7 Hz, 3H, **H7**), 1.51 (d, *J*_{H,P} = 12.0 Hz, 18H, 2 C(CH₃)₃), 1.19 (d, *J*_{H,P} = 12.0 Hz, 18H, 2 C(CH₃)₃). Due to multiple overlapping peaks, the resonances for the ethylene linker of the dtbpe ligand could not be confidently assigned.

³¹P{¹H} NMR (162 MHz, tol-d₈, -50°C) δ 66.1 (s), 51.6 (s).

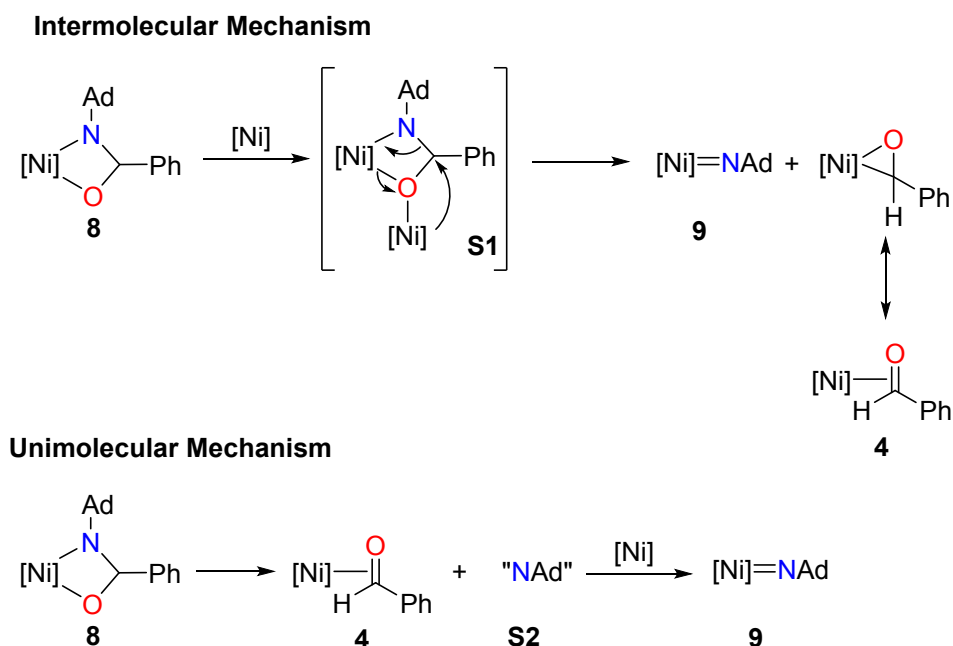
UV/vis (THF; λ_{max} (ε)): 560 nm (1100 M⁻¹ cm⁻¹)

LRMS (EI) 630 [M-H]⁺

III. Mechanistic Scheme

We initially hypothesized that **9** and **4** were formed from one of two likely mechanisms, as outlined below in Scheme S1. In the first option, coordination of an equivalent of (dtbpe)nickel(0) to the O donor atoms of **8** would form bimetallic intermediate **S1**. Subsequent C-N bond cleavage and Ni-C bond formation would then form **9** and **4**. Of note, although we believe that the O atom of **8** is more sterically accessible, we cannot rule out coordination of (dtbpe)nickel(0) to the N atom of **8** based on our current data.

In the second possible mechanism, **8** undergoes a rate-limiting unimolecular fragmentation to form **4** and a reactive nitrene intermediate **S2**, which could be either triplet or singlet spin states. This nitrene could then react with (dtbpe)nickel(0) rapidly to form **9**.



Scheme S1. Possible Intermolecular (above) and unimolecular (below) mechanisms of formation of **4** and **9** from **8**. [Ni] = (dtbpe)nickel.

IV. NMR Spectra

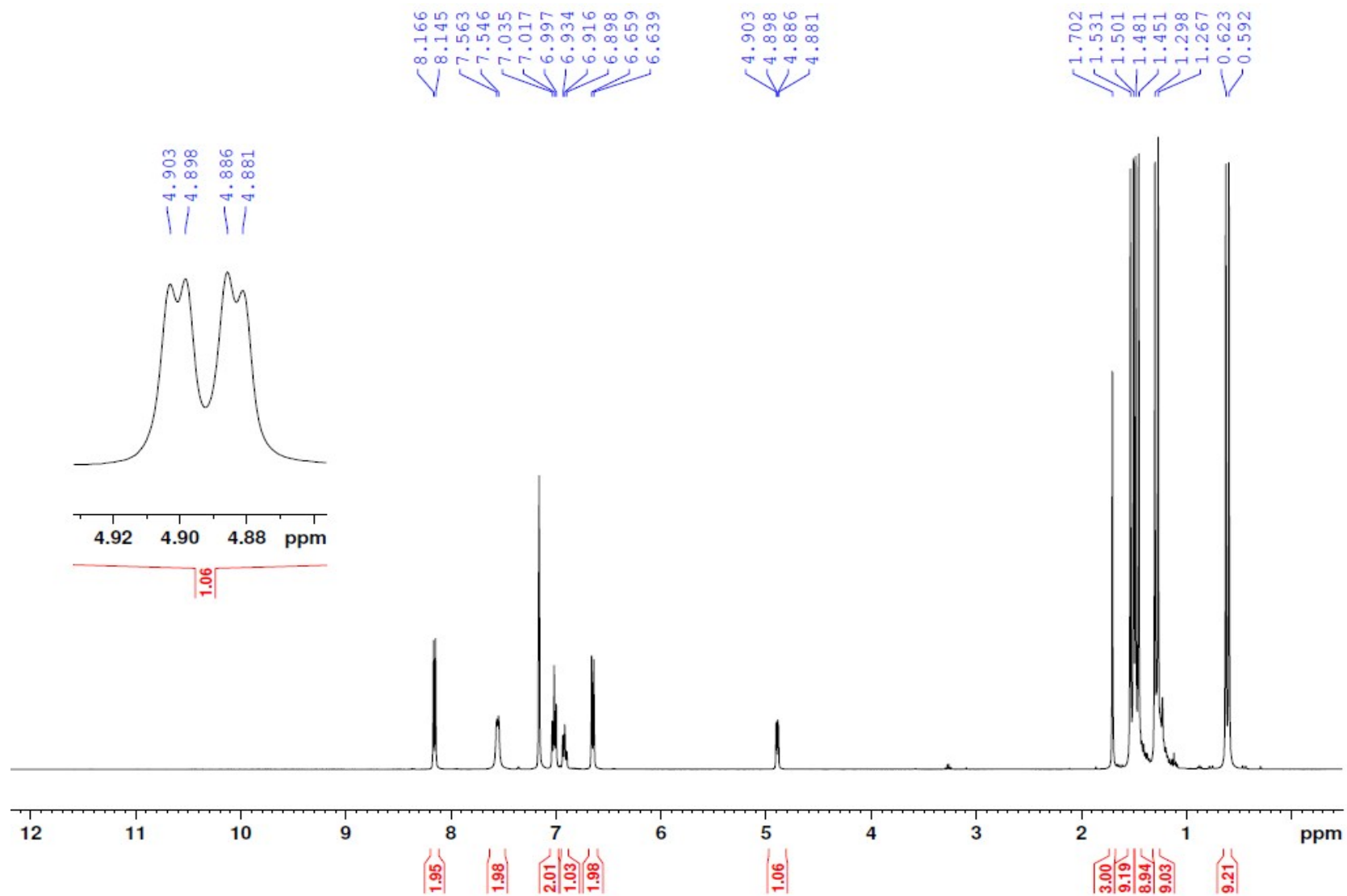


Figure S1. ^1H NMR spectrum (400 MHz, C_6D_6 , 25°C) of **3**. Inset shows **H1** resonance.

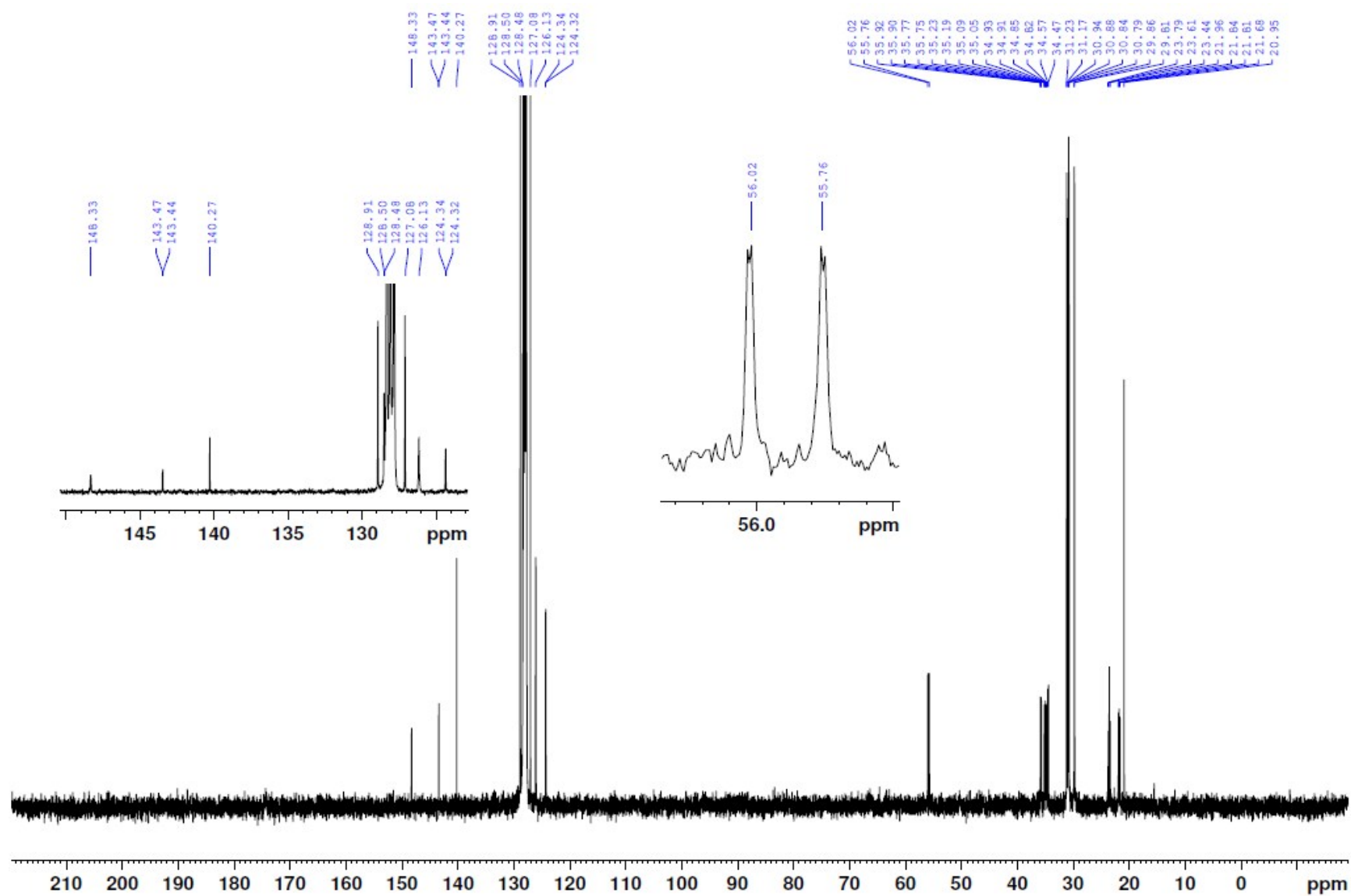


Figure S2. $^{13}\text{C}\{^1\text{H}\}$ NMR spectrum (100 MHz, C_6D_6 , 25°C) of **3**. Left inset shows the aromatic region, the right inset shows the C1 resonance.

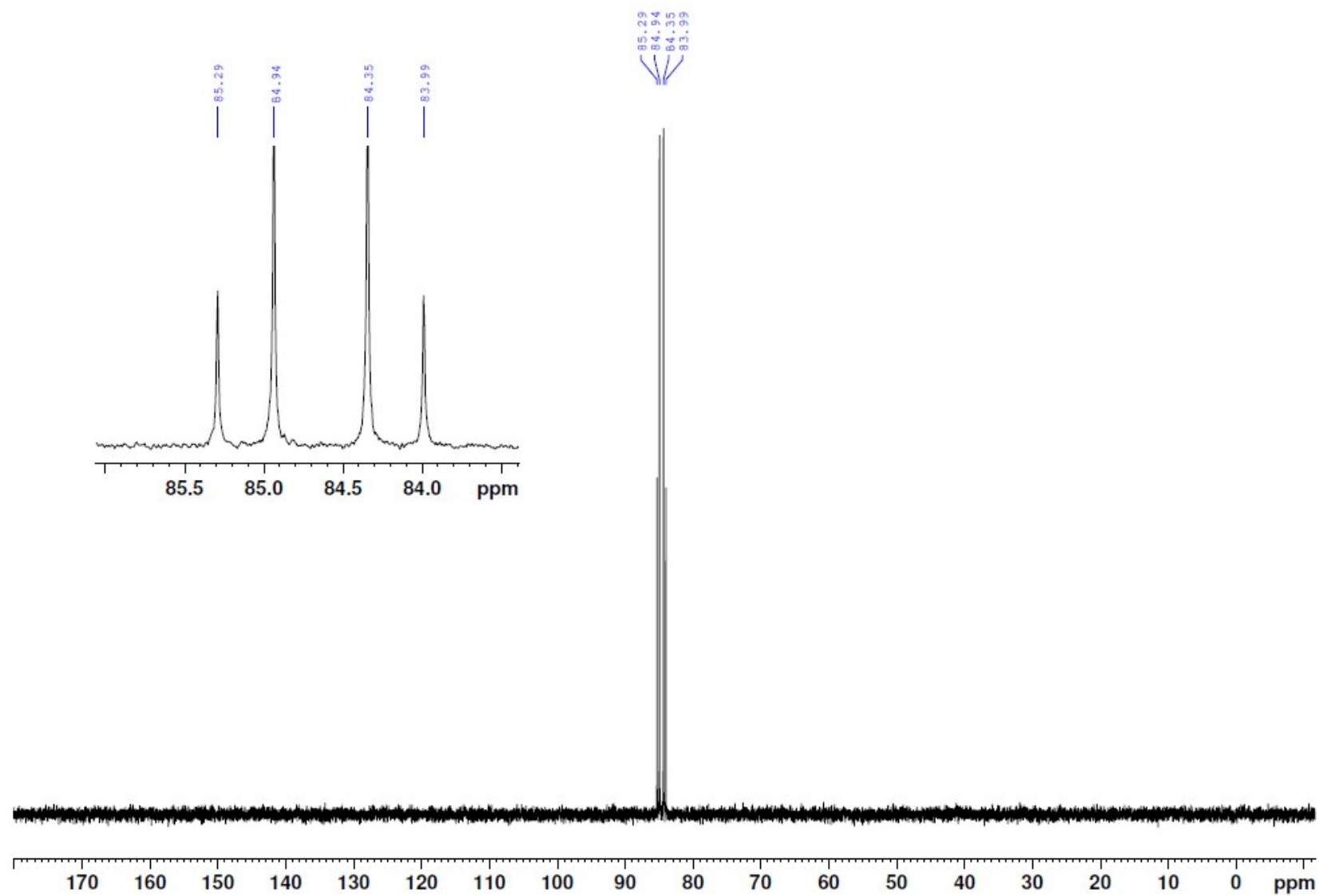


Figure S3. $^{31}\text{P}\{^1\text{H}\}$ NMR spectrum (120 MHz, C_6D_6 , 25°C) of **3**.

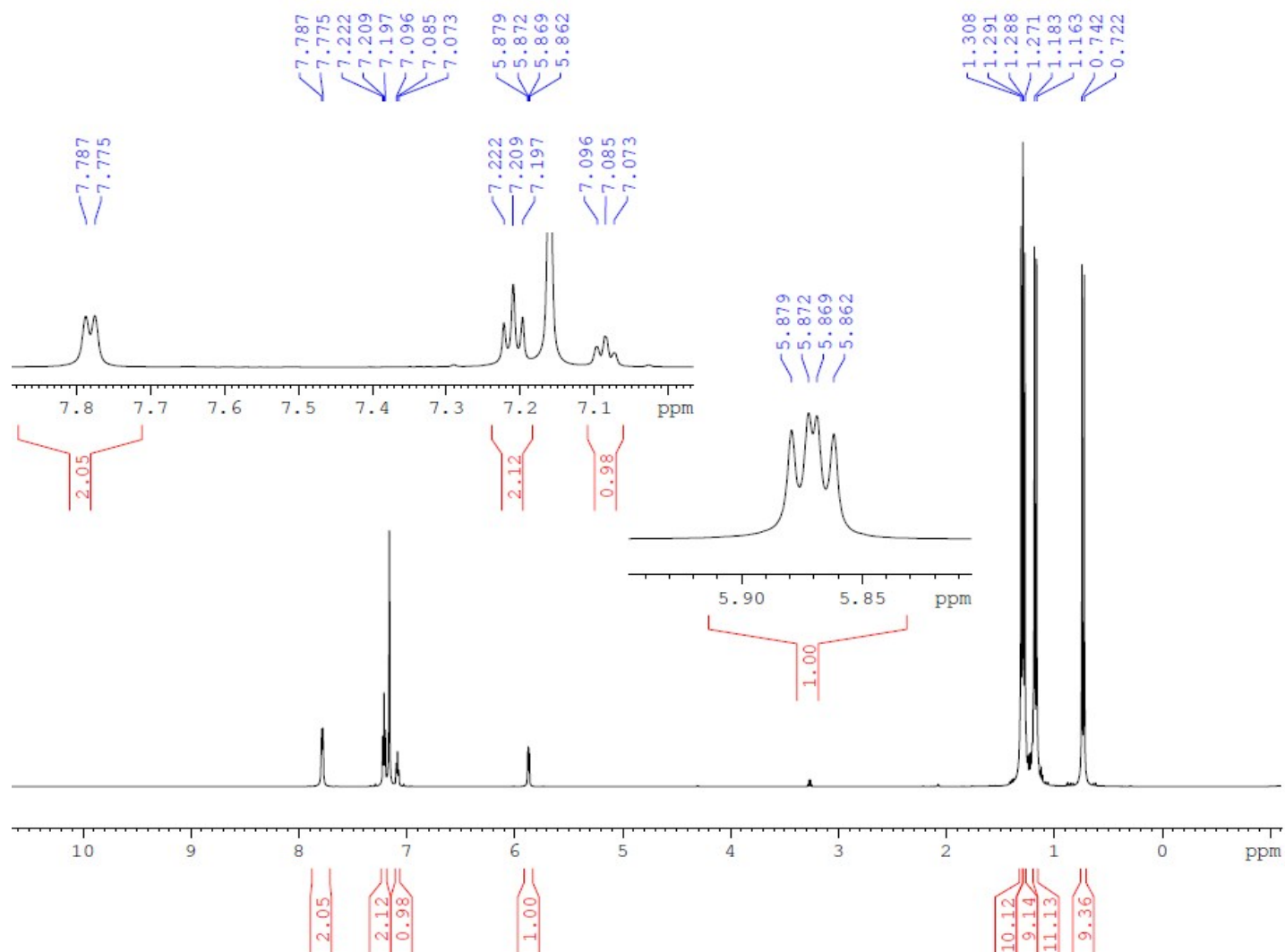


Figure S4. ^1H NMR spectrum (600 MHz, C_6D_6 , 25°C) of **4**. Left inset shows the aromatic resonances, while the right shows the **H1** resonance.

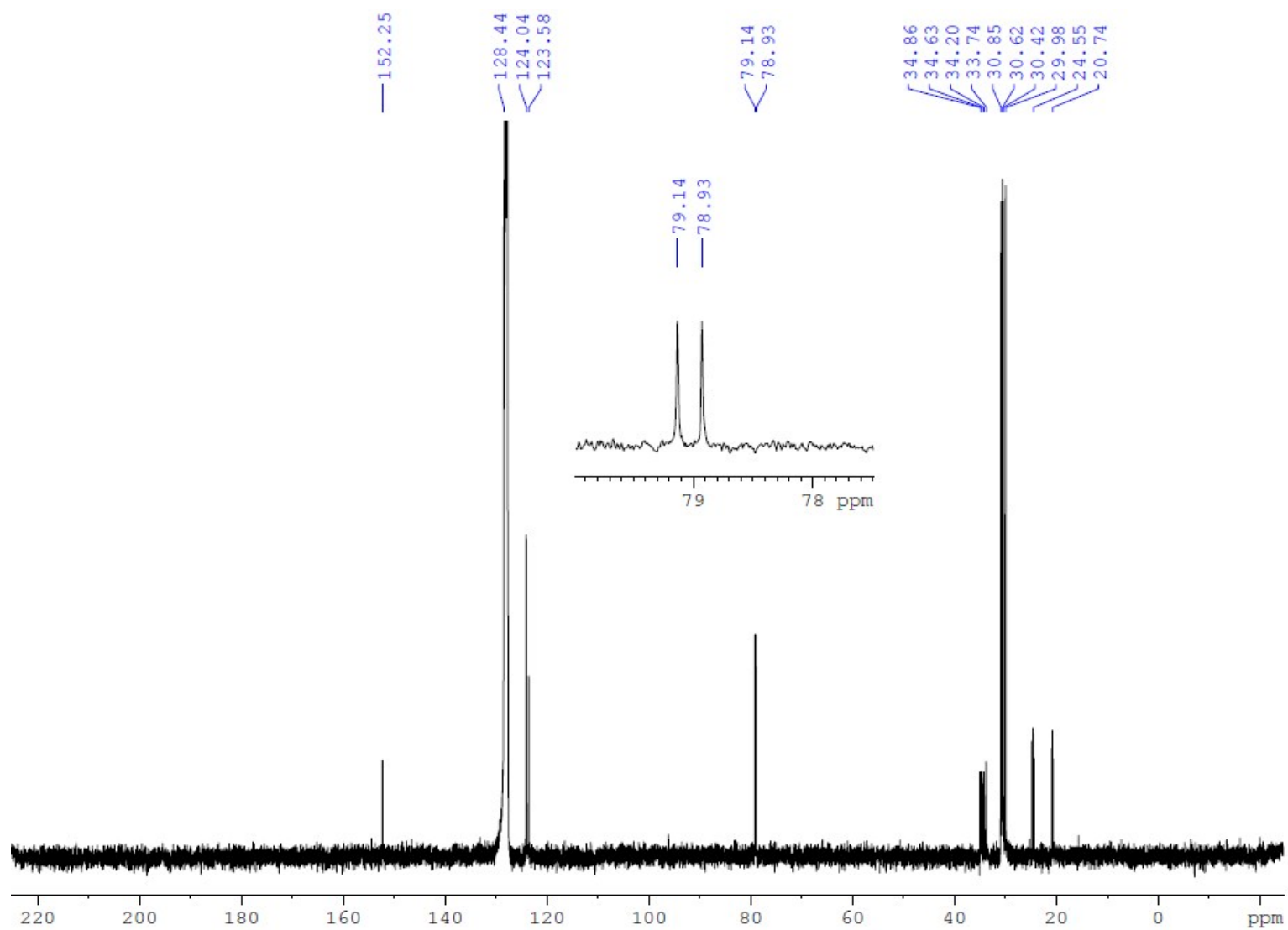


Figure S5. $^{13}\text{C}\{^1\text{H}\}$ NMR spectrum (100 MHz, C_6D_6 , 25°C) of **4**. Inset shows the C1 resonance.

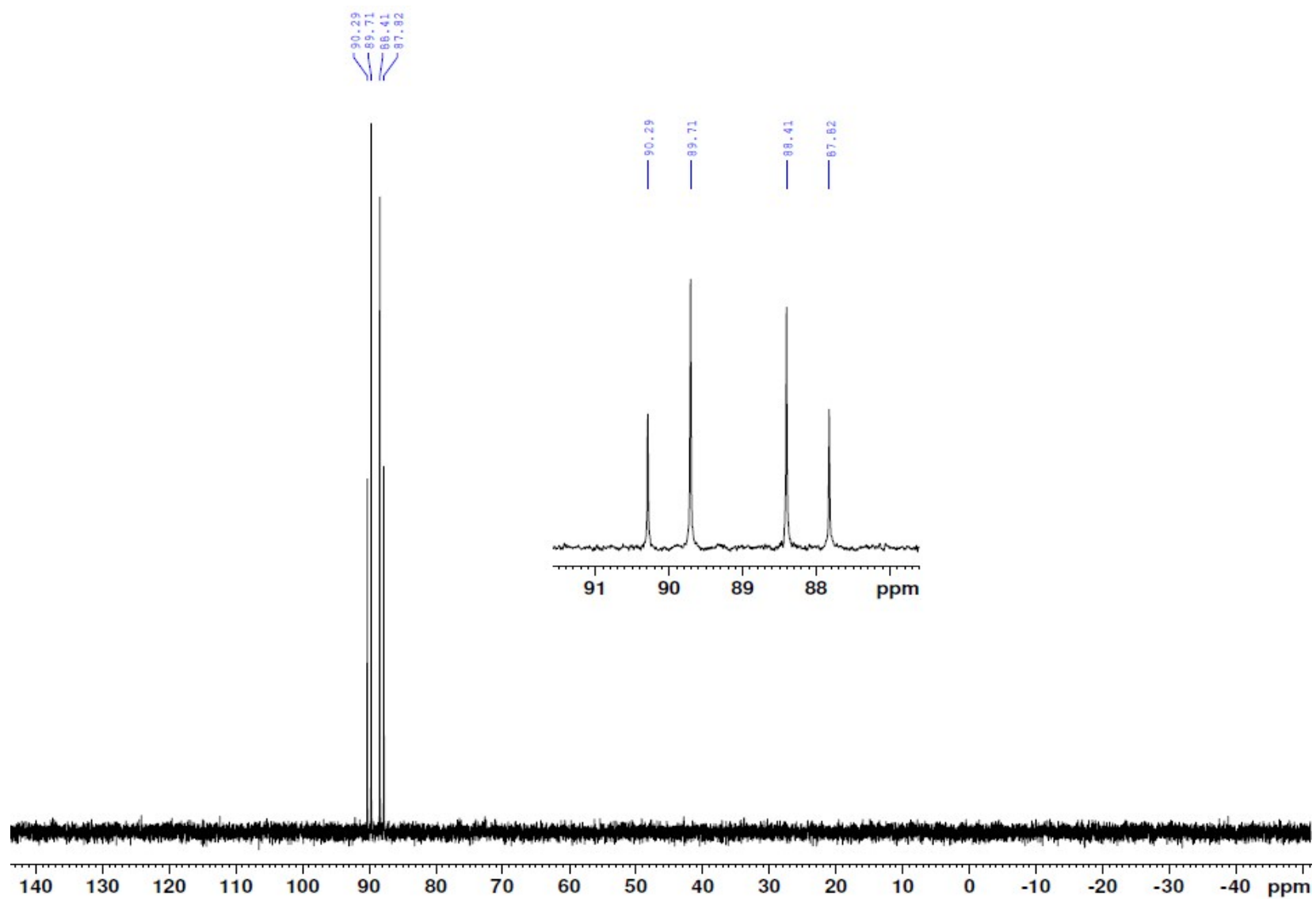


Figure S6. $^{31}\text{P}\{^1\text{H}\}$ NMR spectrum (162 MHz, C_6D_6 , 25°C) of 4.

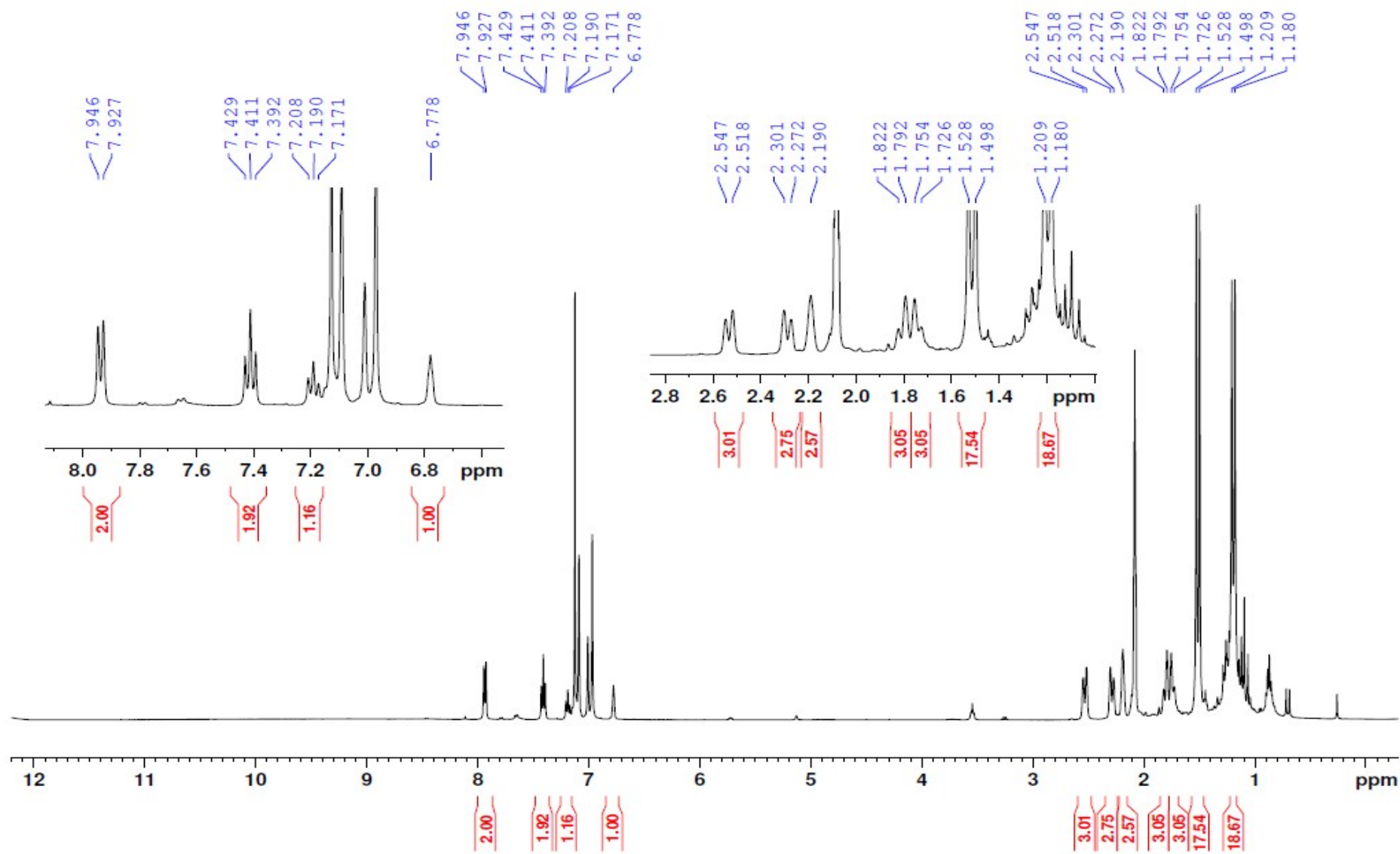


Figure S7. ^1H NMR spectrum (400 MHz, tol-d_8 , 25°C) of **8**. Left inset shows the aromatic region, right inset shows the aliphatic region.

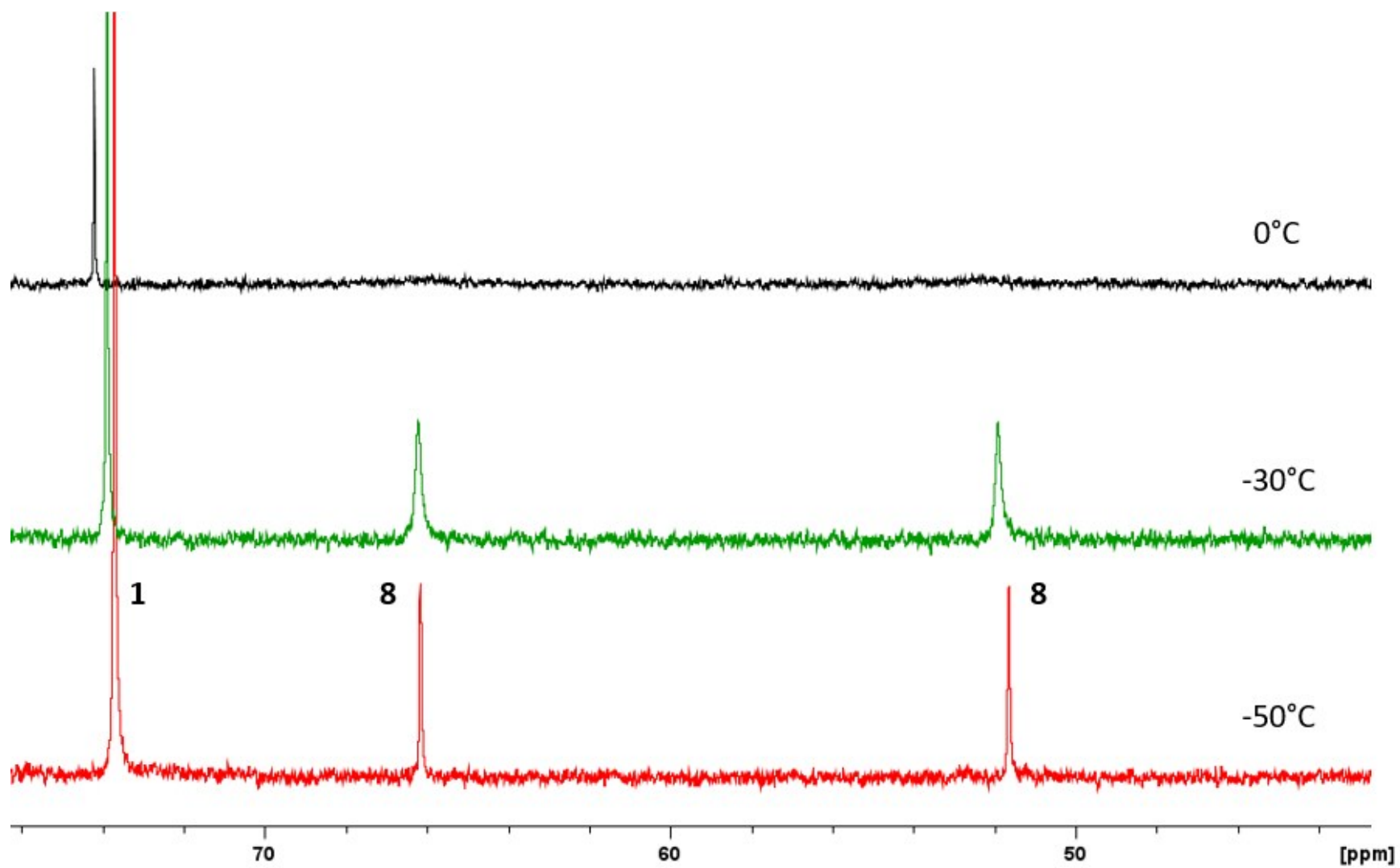


Figure S8. Variable temperature $^{31}\text{P}\{^1\text{H}\}$ NMR spectra of the reaction of **1** with oxaziridine **7** at -50°C (red trace), -30°C (green trace) and 0°C (black trace). The most downfield resonance is due to unreacted **1**.

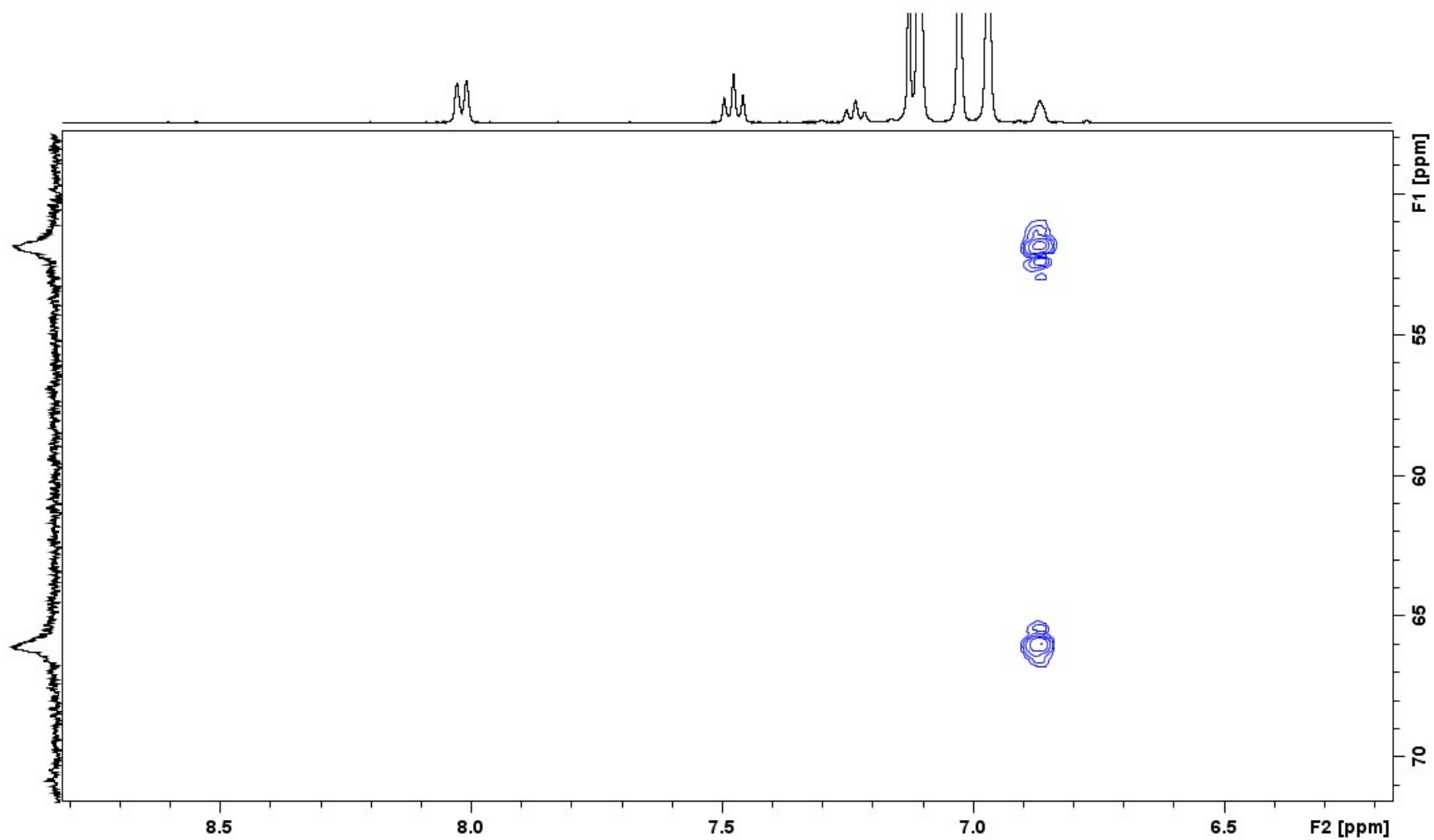


Figure S9. Partial ^{31}P - ^1H HMBC spectrum of **8** at -20°C showing the correlation between the phosphorous resonances and the **H1** resonance.

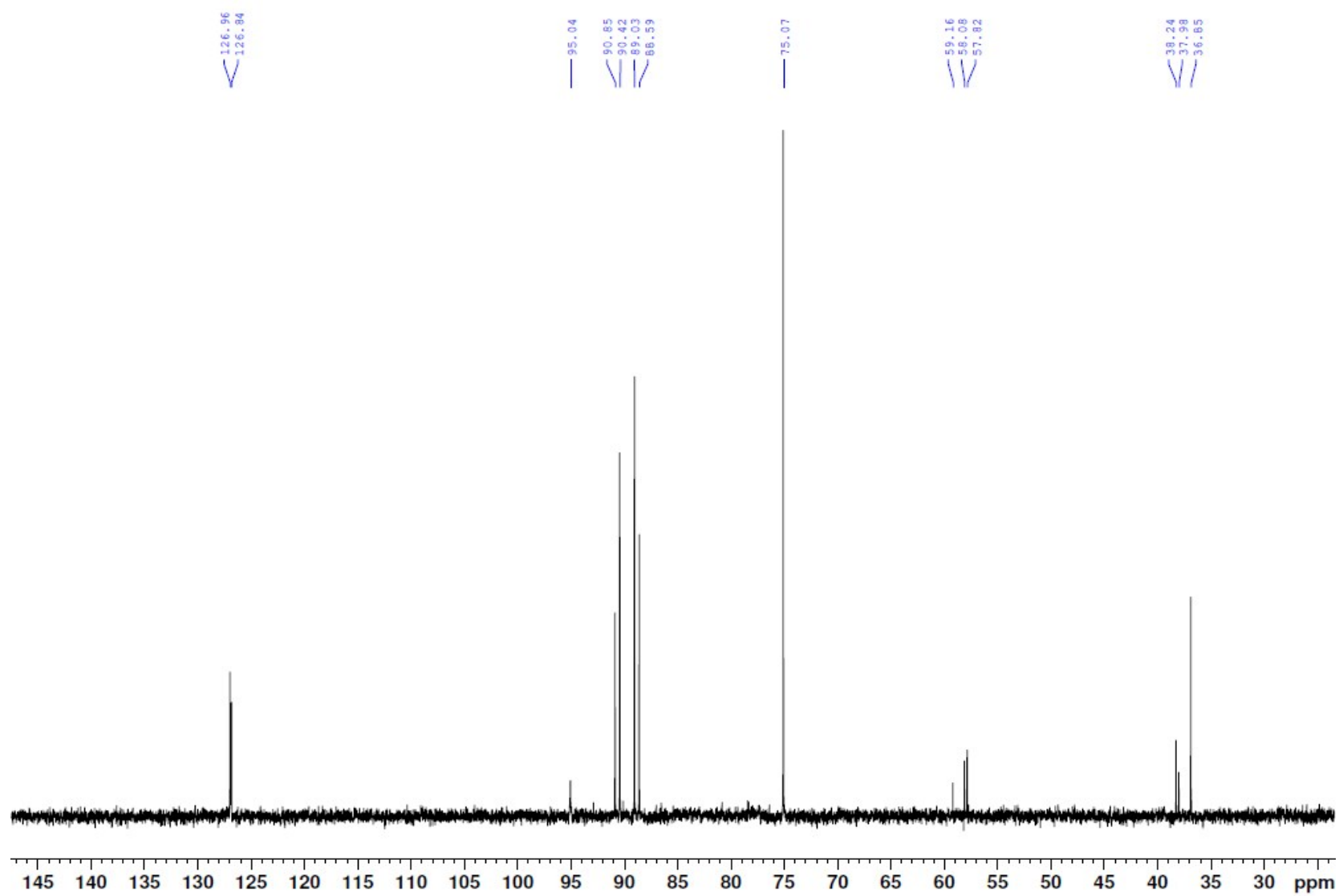


Figure S10. $^{31}\text{P}\{^1\text{H}\}$ NMR spectrum (162 MHz, C_6D_6 , 25°C) of the reaction of **1** with oxaziridine ^{15}N -7.

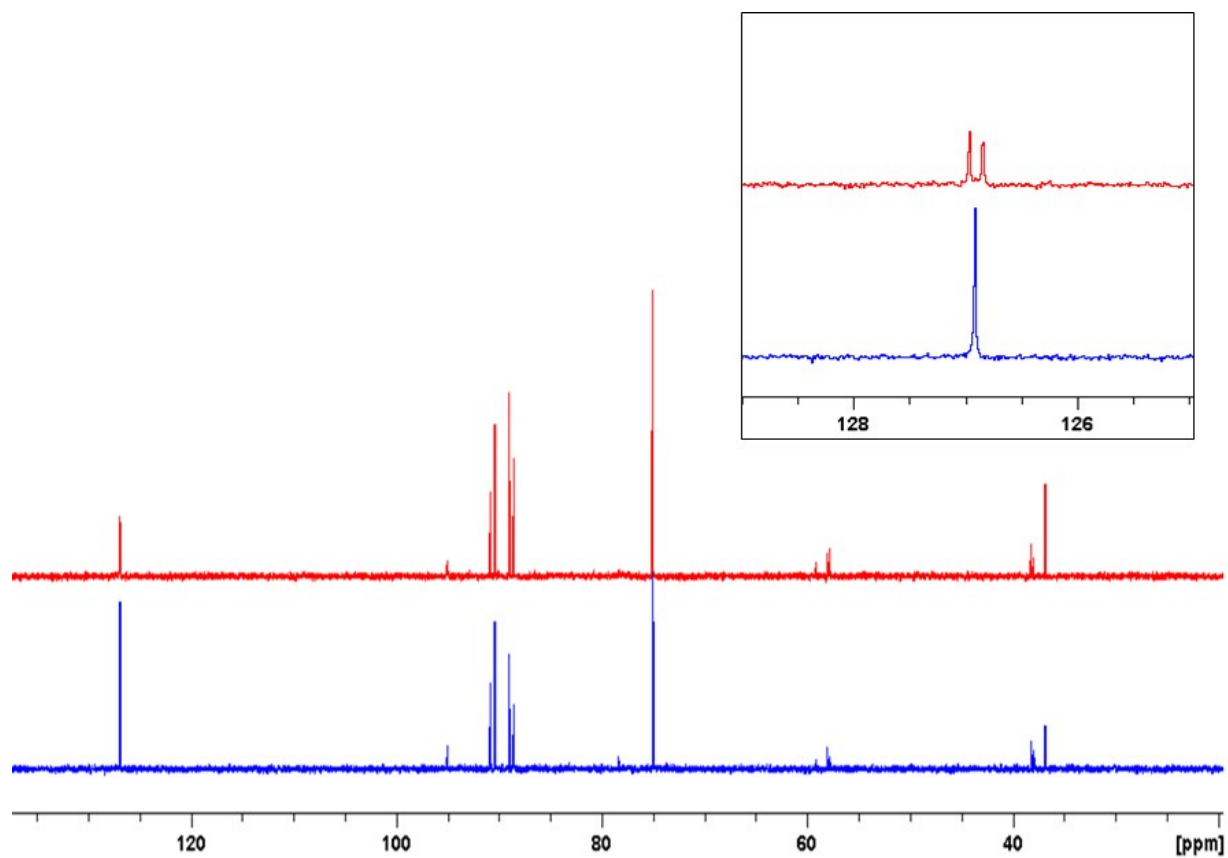


Figure S11. $^{31}\text{P}\{^1\text{H}\}$ NMR spectra (162 MHz, C_6D_6 , 25°C) of the reaction of **1** with ^{15}N -enriched (red trace) oxaziridine-7 and unlabeled **7** (blue trace). Inset shows $^{31}\text{P}\{^1\text{H}\}$ NMR peak of ^{15}N -labelled **9** (red trace) ($^2J_{\text{P,N}} = 19$ Hz) compared to unlabelled **9** (blue trace).

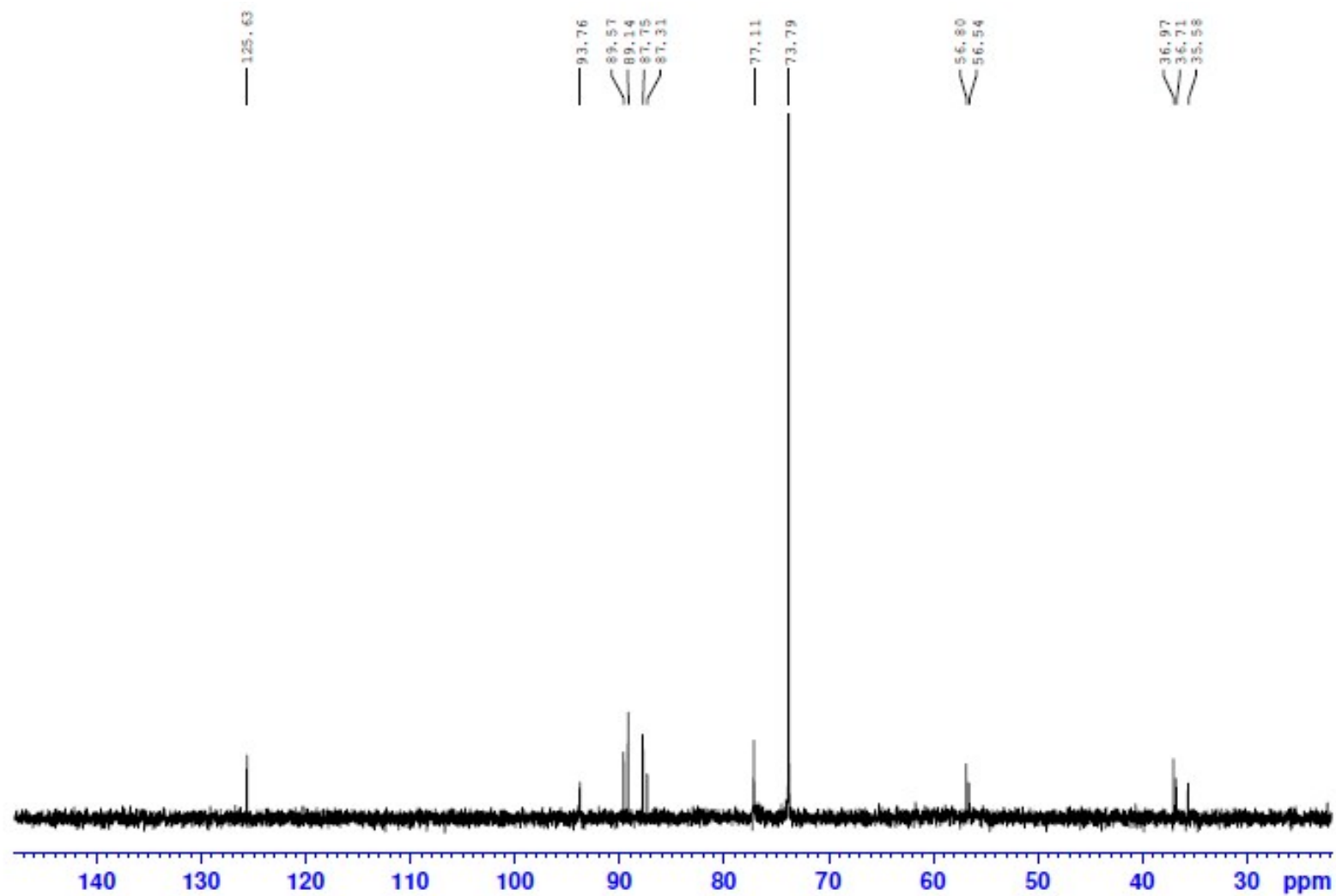


Figure S12. $^{31}\text{P}\{^1\text{H}\}$ NMR spectrum (162 MHz, C_6D_6 , 25°C) of the reaction of **8** with 0.5 equiv. of **1**.

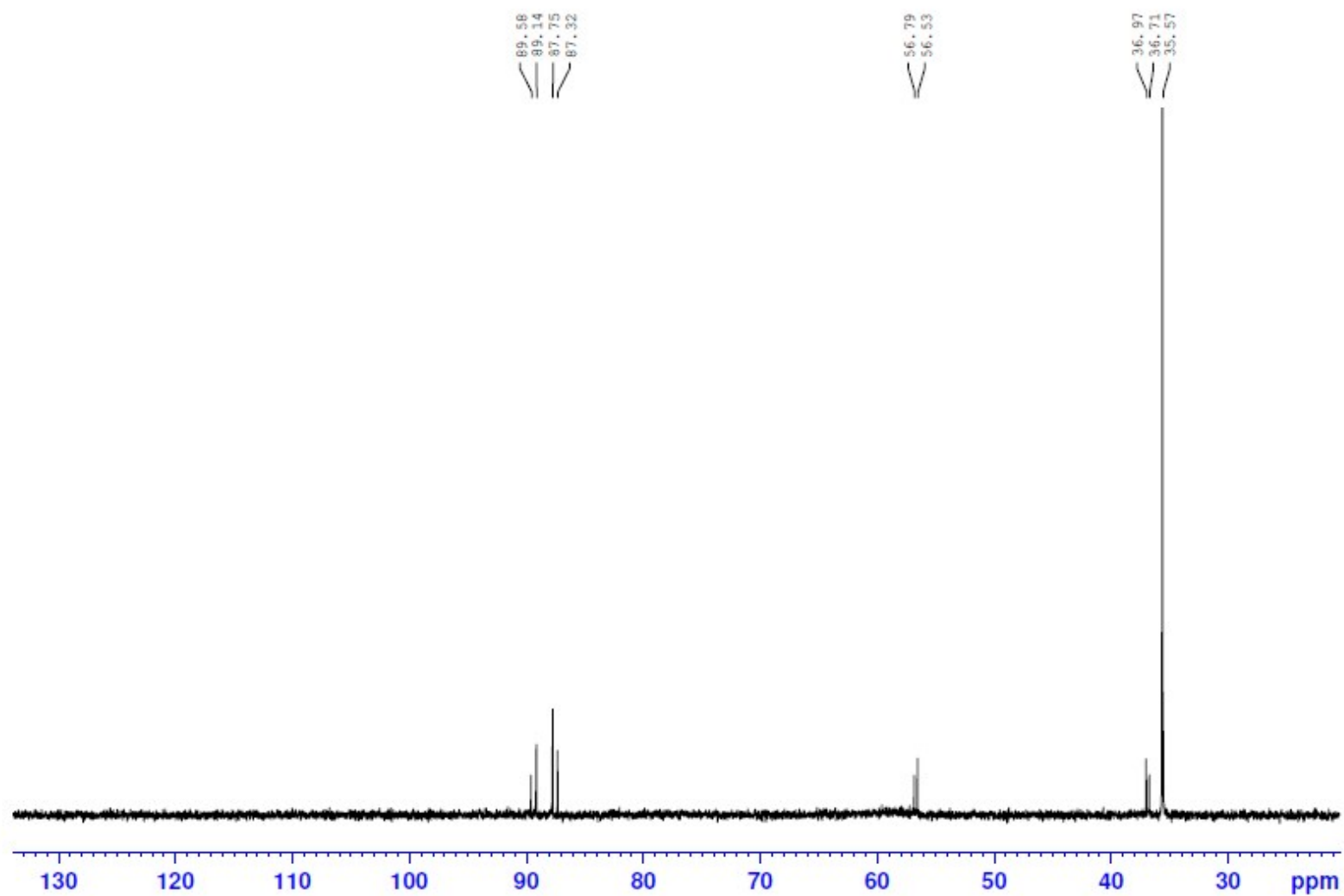


Figure S13. $^{31}\text{P}\{^1\text{H}\}$ NMR spectrum (162 MHz, C_6D_6 , 25°C) of the reaction of **8** with 1.00 equiv. of dtbpe.

V. UV-Vis Spectrophotometry

The following procedure was followed to obtain the absorbance spectrum of **8** – in a glovebox, a solution of **8** (5.00 ml) in THF was prepared using **7** (5.1 mg, 0.020 mmol, 2.0 equiv) and **1** (8.3 mg, 0.010 mmol, 1.0 equiv). After cooling for 30 mins, the deep purple solution was diluted and transferred into an anaerobic cuvette, which was taken out of the glovebox and maintained in an ice-bath. The solution was analyzed from 200-800 nm.

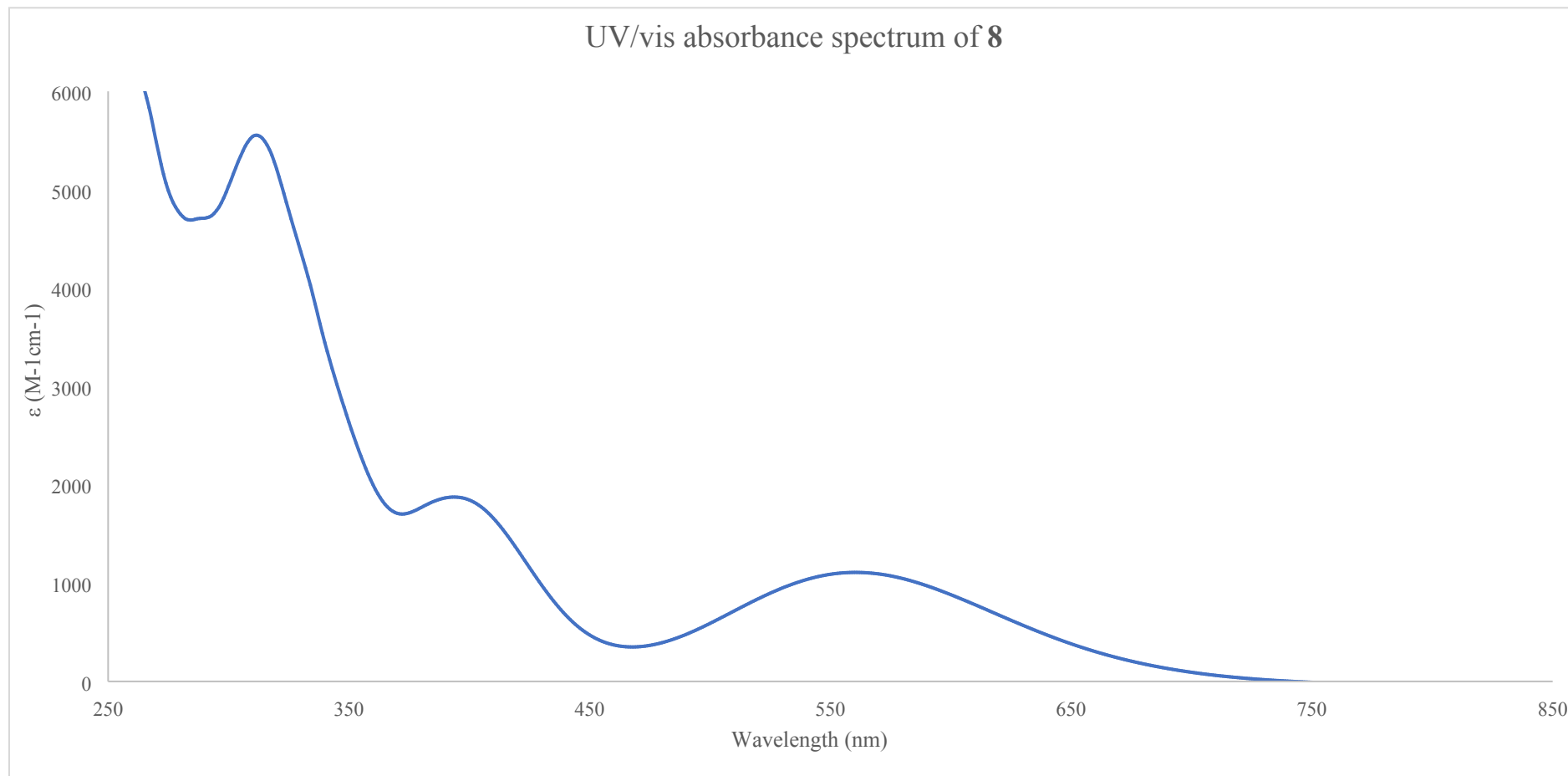


Figure S14. UV-Vis absorbance spectrum of **8** at room temperature.

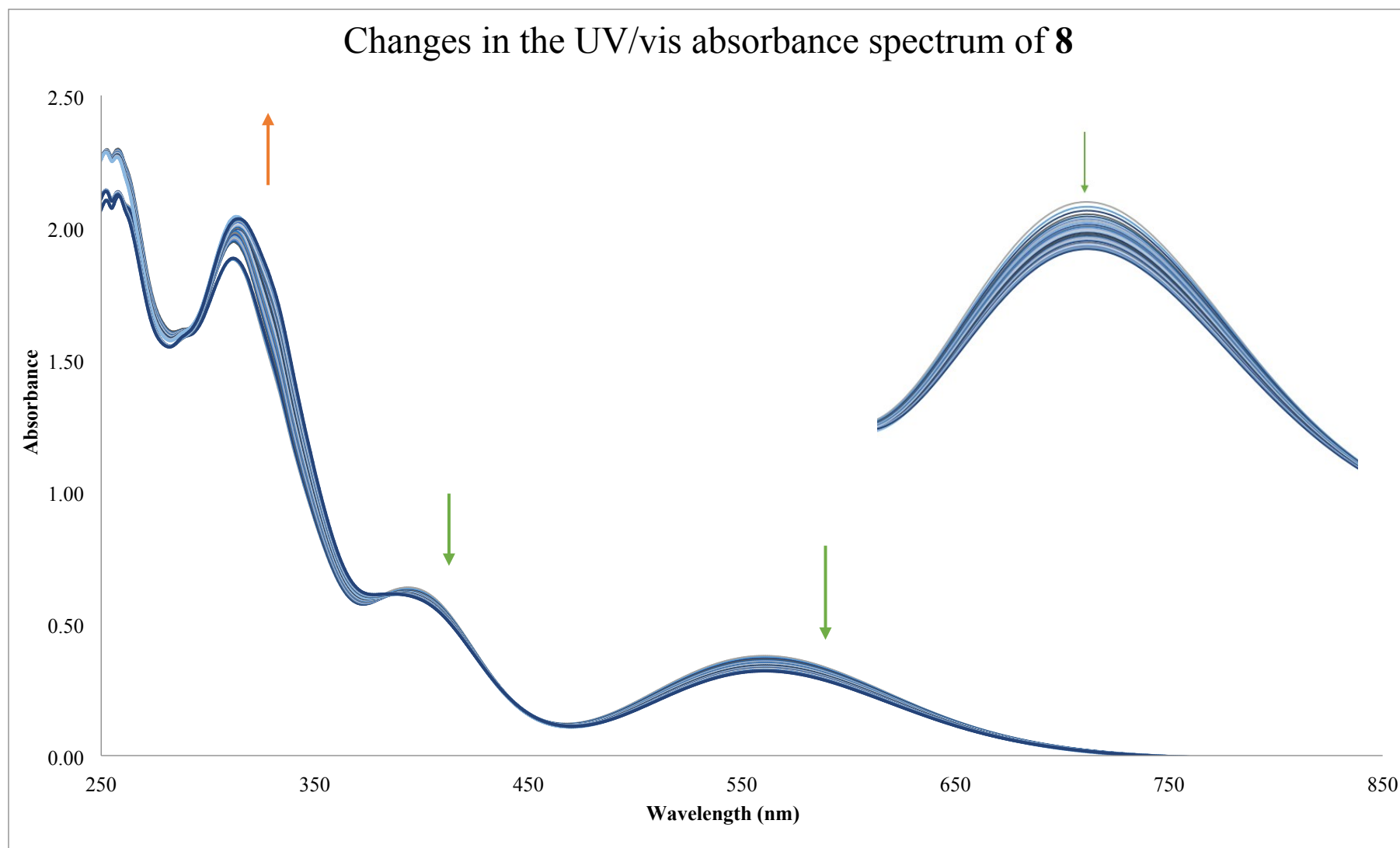


Figure S15 Changes in the UV/vis absorbance spectrum of **8** (initial concentration 0.44 mM, rt, scans every 60 s) over time. Green arrows indicate bands that decrease in intensity. Orange arrow indicates bands that increase in intensity. Inset shows the band at 560 nm.



Figure S16. Appearance of **8** (0.88 M) in THF.

To monitor the decay of **8** with 0.50 equiv of **1**, the following procedure was used – a 4.0 mM standard solution of **8** (5.0 mL) and a 20 mM standard solution of **1** (1.0 mL) were prepared in THF, and cooled in a freezer in the glovebox at $-30\text{ }^{\circ}\text{C}$. **1** (160 μL , 3.2 mmol of Ni) was diluted with THF (3.0 mL) and withdrawn into a syringe with nitrogen in the headspace. **8** (800 μL , 3.2 mmol of Ni, 1.00 equiv) was transferred into an anaerobic cuvette, which was then sealed, removed from the glovebox, and chilled in an ice bath. Before loading the cuvette into the UV-Vis spectrophotometer, **1** was injected into the cuvette, and the absorbance of **8** was monitored at 560 nm over 15 minutes.

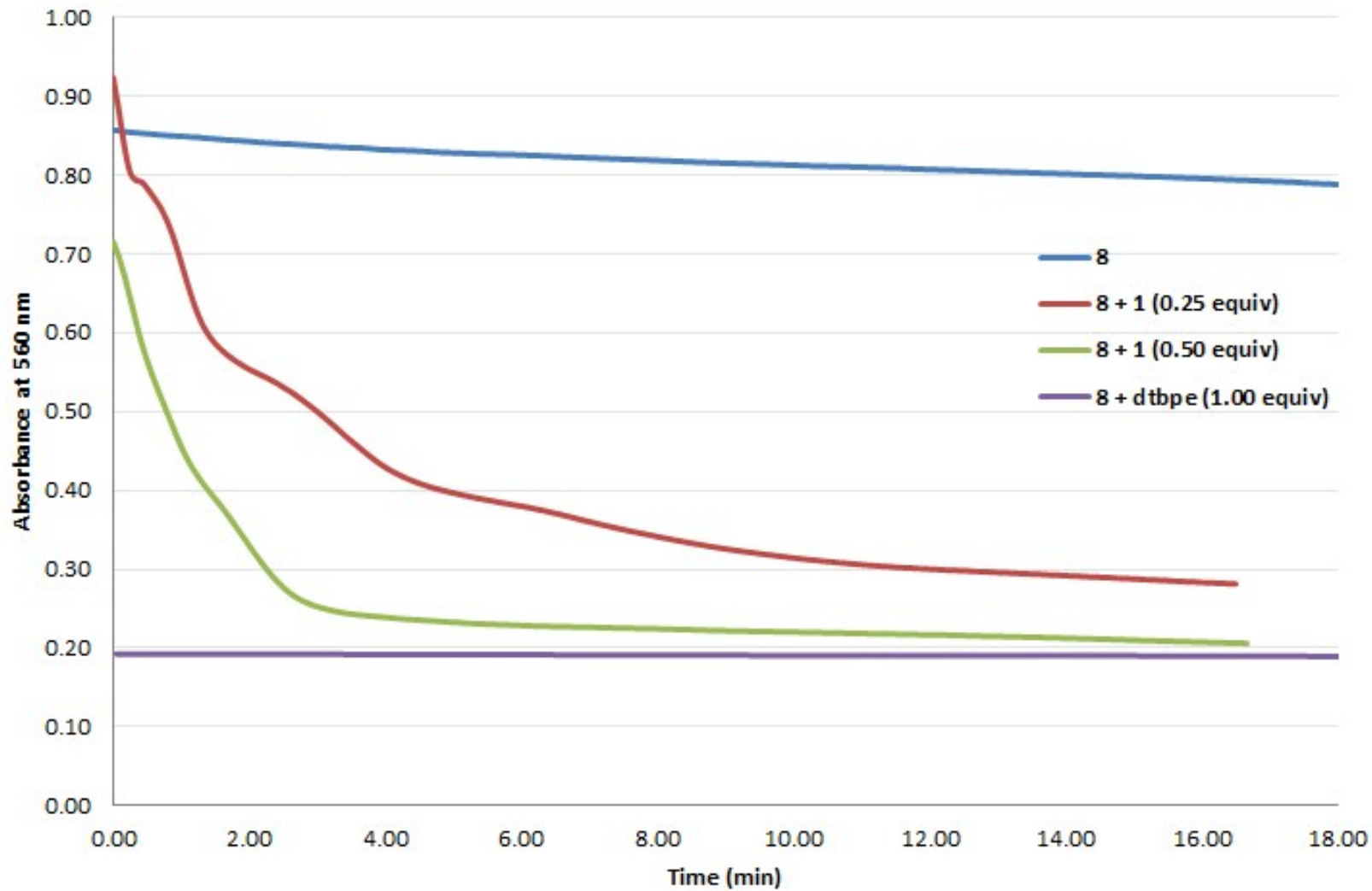


Figure S17. Monitoring the decay of **8** with 0 (blue trace), 0.25 (red trace), and 0.50 (green trace) equiv of **1** by measuring the absorbance of **8** at 560 nm over 15 minutes. Due to the instantaneous reaction of **8** with 1 equiv of dtbpe (purple trace), we were unable to monitor its decay over 15 minutes.



Figure S18. Appearance of a mixture of **8** and **1**, 15 minutes after the addition of **1** (0.50 equiv) to **8**.

VI. X-ray Crystallography

Crystals of **3**, **4**, and **8** were mounted on a glass fiber loop. All measurements were made at 90(2) K, using Mo K α radiation ($\lambda=0.71073$ Å) on a Bruker APEX DUO diffractometer equipped with a TRIUMPH monochromator. The structures were solved by direct methods¹ and refined by full-matrix least-squares procedures on F² (SHELXL-2013)¹ using the OLEX2 interface.² Compound **4** crystallizes with two independent molecules in the asymmetric unit. All hydrogen atoms were placed in calculated positions. For all complexes, non-hydrogen atoms were refined anisotropically.

CCDC **1537039-1537041** contains the supplementary crystallographic data for this paper. These data can be obtained free of charge from The Cambridge Crystallographic Data Centre *via* www.ccdc.cam.ac.uk/data_request/cif.

References:

1. G.M. Sheldrick *Acta Cryst.* 2008, **A64**, 112-122.
2. O.V. Dolomanov; L.J. Bourhis; R.J. Gildea; J.A.K. Howard; H. Puschmann *J. Appl. Cryst.* 2009, **42**, 339-341.

Table S1. Crystallographic data for **3**, **4** and **8**

Compound	3	4	8
Empirical formula	C ₃₂ H ₅₃ INNiO ₂ P ₂ S	C ₂₅ H ₄₆ NiOP ₂	C ₃₅ H ₆₁ NNiOP ₂
Formula weight	636.46	483.27	632.52
Temperature/K	90(2)	90(2)	90(2)
Crystal system	monoclinic	monoclinic	monoclinic
Space group	Cc	P2 ₁ /c	P2 ₁ /n
a/Å	15.205(2)	15.728(3)	11.3153(15)
b/Å	16.403(3)	20.763(4)	17.650(2)
c/Å	13.947(2)	16.376(3)	17.536(2)
α/°	90	90	90
β/°	102.508(5)	96.899(4)	103.453(3)
γ/°	90	90	90
V/Å ³	3396.0(9)	5309.3(18)	3406.0(8)
Z	4	8	4
ρ/ g/cm ⁻³	1.245	1.209	1.2334
μ/ mm ⁻¹	0.755	0.865	0.691
F(000)	1368.0	2096.0	1378.6
Crystal size/ mm ³	0.27 × 0.18 × 0.12	0.25 × 0.18 × 0.09	0.24 × 0.16 × 0.11
Radiation	MoKα (λ = 0.71073)	MoKα (λ = 0.71073)	MoKα (λ = 0.71073)
2θ range for data collection/°	3.7 to 60.156	2.608 to 60.334	3.32 to 58.42
Index ranges	-21 ≤ h ≤ 19, -23 ≤ k ≤ 22, -19 ≤ l ≤ 19	-22 ≤ h ≤ 22, -28 ≤ k ≤ 29, -23 ≤ l ≤ 23	-15 ≤ h ≤ 15, -23 ≤ k ≤ 24, -14 ≤ l ≤ 24
Independent reflections	7937 [R _{int} = 0.0472, R _{sigma} = 0.0597]	15653 [R _{int} = 0.0489, R _{sigma} = 0.0363]	9175 [R _{int} = 0.0415, R _{sigma} = 0.0374]
Data/restraints/parameters	7937/2/365	15653/0/555	9175/0/376
Goodness-of-fit on F ²	1.000	1.012	1.025
R [I>=2σ(I)] (R1, wR2)	R ₁ = 0.0361, wR ₂ = 0.0756	R ₁ = 0.0330, wR ₂ = 0.0799	R ₁ = 0.0359, wR ₂ = 0.0859
R (all data) (R1, wR2)	R ₁ = 0.0449, wR ₂ = 0.0790	R ₁ = 0.0464, wR ₂ = 0.0863	R ₁ = 0.0488, wR ₂ = 0.0927
Largest diff. peak/hole / (e Å ⁻³)	0.87/-0.38	1.94/-0.71	1.39/-0.36

$$R1 = \Sigma ||F_o| - |F_c|| / \Sigma |F_o|; wR2 = [\Sigma(w(F_o^2 - F_c^2)^2) / \Sigma w(F_o^2)^2]^{1/2}$$